Analytical Study of the Failure Modes and Capacity of the Sequoyah Containment

Joel D. Miller, David B. Clauss
Sandia National Laboratories, Albuquerque, NM USA

INTRODUCTION

Sandia National Laboratories, in its role as manager of the Containment Integrity Programs for the United States Nuclear Regulatory Commission (NRC), has developed analytical techniques for predicting the performance of light water reactor steel containment buildings subject to loads beyond the design basis. The analytical techniques are based on experience with large scale steel containment model tests. Results of the model tests provided important insights into the structural response of steel containments and experimental validation of the analytical methods. The methodology for analyzing steel containments has advanced to the point that the NRC asked Sandia to demonstrate these analytical techniques on an actual steel containment building under hypothetical conditions of severe accident loading. The objective of the analysis was to determine the actual pressure capacity and the mode, location, and size of failure, based on a functional definition of failure.

The Sequoyah Unit 1 containment building was selected for the analysis for several reasons. It has a steel ice-condensor containment, which was similar in many respects to the 1:8-scale model that was tested by Sandia (Koenig, 1986). Sequoyah is one of the reference plants in the NUREG-1150 study (USNRC, 1987) and has been analyzed repeatedly; thus it is a useful benchmark for advances in analytic capabilities. Finally, it was shut down at the time the study was initiated, which allowed for first-hand inspection of the containment by the analysts.

METHODOLOGY

Basic steps in the analysis procedure include definition of the potential failure modes, selection of the evaluation criteria, design and load definition, structural response calculations, and interpretation of results. The analysis procedure is documented more fully in Clauss and von Riesemann, 1988. Analysis of only one failure mode, general shell rupture, will be presented here. Discussion of other failure modes is available in Miller and Clauss, 1988.

Two load cases were considered in the study: slow pressurization at ambient temperature (for comparison with previous analyses) and slow pressurization at temperatures corresponding to that of saturated steam at pressure. Each load case was analyzed with static, large-deformation elastic-plastic finite element models of the containment building, using the K.2 version of the structural analysis program MARC (MARC Analysis Research Corp., 1983).

For each load case two separate three-dimensional geometric models were employed: a 4° circumferential model covering the full height of the containment over a "typical" symmetric section (Fig. 1), and a 90° model covering one quarter of the circumference of the structure but not its full height (Fig. 2). The purpose of the latter model was to evaluate explicitly the behavior due to the geometry at a penetration, which could not be represented in the 4° model. The 4° model provides the free field response of the structure and also a direct comparison to the earlier numerical analyses, which were primarily axisymmetric.

CONTAINMENT GEOMETRY AND PREVIOUS ANALYSES

The Sequoyah Unit 1 containment is a right circular cylinder capped by a hemispherical dome, and is constructed entirely with A516 Gr 60 steel. Twelve courses of approximately 10 feet high by 30 feet wide plates comprise the cylindrical shell, with each plate course decreasing in thickness with gain in elevation, from 1-3/8 inches at the basemat to 1/2 inch at the springline. The hemispherical dome is composed of four circumferential courses of plates that increase in thickness from 7/16 inch at the springline up to 15/16 inches at the apex. The floor is embedded within several feet of concrete and is considered rigid compared to the freestanding cylindrical walls and dome. Welded to the shell's exterior surface is a web of horizontal and vertical (at 4° spacing) stiffening members and other miscellaneous structures. At penetration locations, the shell plate thickness increases to 1-1/2 inches and the stiffening members are "rerouted" to bypass the penetration. The 4° model included the "typical" shell plates and both the horizontal and vertical stiffening members, while the 90° model was specifically centered at the 293° azimuth position and included the actual shell plates, horizontal stiffeners, and the thicker replacement and insert plates at particular penetrations.

Previous analytical studies of the Sequoyah containment (Greimann et al, 1984) were made either with axisymmetric finite element analyses or by hand. The capacity of the containment shell was estimated to range from 27 to 67 psig, with various failure mechanisms and criteria postulated. The original design basis of the containment was for internal pressure of 10.8 psig.

MODELING CONSIDERATIONS

Pressure loads were applied statically to simulate the slow build-up of gas within the containment. The net pressure load was specified to act as a uniformly-distributed "follower" force, remaining normal to the interior element surface of the containment shell as it deformed. The pressure load was applied in increments up to or beyond the predicted failure pressure. For the elevated-temperature load case, the temperature was increased uniformly along with the pressure increments to correspond to temperature properties of confined saturated steam. At 50 and 75 psig, for example, the temperature equaled 298° and 320° F, respectively.

The nodes on the vertical edges of the finite element models were assigned symmetry compatible boundary conditions: these nodes were constrained against circumferential displacements but otherwise unrestricted from movement. All degrees of freedom were constrained along the bottom edge of the 4° model to simulate the rigid connection at the basemat. Since the 90° model did not cover the full height of the structure, traction forces along the upper boundary represented the meridional membrane forces. The traction forces were specified to remain tangent to the meridional curvature of the shell and normal to the circumferential curvature at each boundary node. The traction forces were increased in direct proportion to the increments of the internal pressure load. A constraint on the vertical displacement along lower boundary of the 90° model was required to resist the traction forces.

Piecewise-linear representations of the work-hardening behavior of A516 Gr 60 steel were used for the ambient temperature analysis of each model. Thickness-specific properties from certified test reports of the Sequoyah steel were used for the 90° model at ambient temperature (Fig. 3), while the 4° model analysis was based on averaged material test data from the 1:8-scale test conducted at Sandia, since the certified test report data had not yet been received. Averaged test data also provided the basis for the representation of material properties at elevated temperatures and was not specific to material thickness for the latter calculations. The data input for the elevated-temperature work-hardening relationship (Fig. 4) did not include yield plateaus, since interpolation between the curves at that point of change in slope, as well as temperature rise, caused convergence difficulties for the program. In all cases, the same large displacement, plasticity with isotropic work hardening constitutive relations based on the von Mises yield criterion were employed. Each model consisted entirely of eight-node-quadrilateral multi-integration layered shell elements.

SHELL FAILURE CRITERION

The finite element structural response calculations must be interpreted in terms of a failure criterion in order to be meaningful. The failure criterion assumed for the general shell rupture mode can be expressed as:

$$\epsilon_{pc} \geq \epsilon_u / \mathbf{K}$$

where ϵ_{pc} is the peak calculated equivalent membrane strain, ϵ_u is the ultimate strain (strain at maximum load from a uniaxial tensile test), and **K** is the product of various knockdown factors for the analysis. The knockdown factors are associated with such considerations as the relative level of sophistication of the finite element analysis, the differences between information on the structure available to the analyst and the actual construction, and variations in the material property data. The level of sophistication of a finite element calculation is determined by the amount of detail and completeness of the geometry, the element size, the appropriateness of boundary conditions, and other assumptions that the analyst must make. The finite element models are based on "as-built" design drawings of the structure, which may not correspond exactly to the finished containment. Material property data were obtained from uniaxial tensile tests; elongation data varied as a function of the gage length.

For the 4° model of the containment, which does not include any asymmetric features or effects such as strain concentrations due to thickened insert plates at penetration locations, the knockdown factor associated with sophistication level is assumed to range from 2 to 5, with a median estimate of 3. These values are based on the previous experience with scale model analysis and testing. Because the 90° model explicitly accounts for the strain concentration effect at a penetration, the knockdown factor for the second model is based primarily on the element size. In order to account for strain gradient effects and the relatively larger sized elements used in this model, a knockdown factor of 1.25 is assigned to the 90° model. An additional factor which is the same for both models relates to the uncertainty between the documented and actual construction. For both models, this design confidence factor is proposed to range from 1 to 1.25. The mean estimate is 1.1. Therefore, the total knockdown factor **K** to be applied to the 4° model could be as low as 2 or as high as 6.25, with an average value of 3.3. **K** for the more explicit 90° model is between 1.25 and 1.56, with a mean value of 1.4.

The ultimate strain is assumed to be 15%, which was the value measured for the A516 Gr 70 steel used in the 1:8-scale test (Reese and Horschel, 1985). The application of knockdown factors to the ultimate strain means that failure is assumed to be imminent when the peak calculated strain exceeds 4.5% (the mean adjusted level) in the 4° model, although failure as predicted by this model could occur between peak calculated strain values as low as 2.4% or as high as 7.5%. A more narrow range of failure is predicted by the more explicit second model. For the 90° model, the calculated peak strains must be between 9.4% and 12% for failure to be assumed. The mean failure value in the second model is 10.7%.

FINITE ELEMENT RESULTS AND INTERPRETATION

The free field response of the containment was calculated using the 4° model. The overall behavior at elevated temperature was qualitatively similar to the response for the ambient temperature case, although different constitutive relations were used for work-hardening of the steel for the different cases. The effect of increasing the temperature was to decrease the strength of the steel (although ductility of the steel is increased), and to consequently lower the pressure capacity of the containment shell. At ambient temperature, yielding of the steel first took place at about 42 psig internal pressure although significant displacement and strain were not apparent until the load increased beyond 65 psig. The maximum displacements occurred in the upper course of 5/8-inch thick plate while the dome expansion was predominantly uniform. Virtually no displacement was measured for the two lowest and thickest plate courses. At a pressure of approximately 88 psig, the maximum radial displacement in the 5/8-inch plates was greater than 30 inches and the strain level exceeded 5% in the 5/8-, 1/2-, and 7/16-inch plates. The deformed shape of this model at a high internal pressure is shown in Figure 5. With pressure and temperature loads acting simultaneously, the same large displacement and strain levels were reached, but at pressure levels 85–90% of those for the ambient temperature case. This correlates approximately with the decrease in ultimate strength of the steel at the elevated temperatures. Localized yielding in the elevated temperature model occurred almost immediately, at the fixed base of the model, due to the large initial temperature increase up to 215° F at 1.0 psig. The onset of generalized plasticity and large displacements with increased load did not begin until the pressure load had reached about 52 psig at 300° F.

The effect of thick insert plates around penetration locations was accounted for directly in the 90° model calculations. Again, the response was qualitatively similar for both the ambient and elevated temperature load cases. The areas of maximum strain occur near the springline in the thinner plates adjacent to the thicker insert plates, as shown in Figure 6. Deformation throughout this model was much less than in the free field model due to the presence of the stiff insert plates; a maximum displacement value of 23 inches was recorded at a strain level of 12%. Simultaneous thermal and pressure loading caused a loss of 5–10% of the ambient temperature pressure capacity.

In order to predict general shell failure from each model, the strain values from the most highly strained locations were plotted against the pressure load (Fig. 7). Since the failure criterion is based on adjusted values of the peak calculated strains, the pressure levels bounding the failure prediction are found directly. No adjustment in the failure strains are made for the slight increase in ductility of the steel at temperature, since the steep slopes of the resulting curves at these pressure levels preclude a significant increase in the pressure capacity. The predicted failure levels are listed in Table 1.

CONCLUSIONS

General failure of the containment shell is predicted for a fairly narrow range of pressures and temperatures. The range of predicted failure is significantly greater than that shown by previous analyses. It is concluded that thermal effects do not change the overall response of the structure or the general shell failure mode and might even be accounted for by simply adjusting the material property data in an ambient temperature analysis to reflect the reduction in strength of the mechanical properties of the steel at higher temperatures. Not all possible failure modes were presented here, and it may be possible that a different mode of failure could occur below the pressure levels attained in this analysis. Nonetheless, the analysis of the Sequoyah containment building demonstrates that the methodology for evaluating steel containment structures, even under extreme loading conditions, is well advanced. The results from this study cannot be generalized to other containment buildings. However, the methodology exists to analyze any steel containment structure subject to loads beyond the design basis.

ACKNOWLEDGEMENT

This work was supported by the U.S. Nuclear Regulatory Commission and performed at Sandia National Laboratories which is operated for the U.S. Department of Energy under Contract Number DE-AC04-76DP00789.

REFERENCES

Koening, L. N., (1986). The Test of a Large Steel Containment Model. NUREG/CR-4216, SAND85-0790, Sandia National Laboratories, Albuquerque, New Mexico.

U. S. Nuclear Regulatory Commission, (1987). Reactor Risk Reference Document. NUREG-1150.

Clauss, D. B., and von Riesemann, W. A. (1988). Analytical Approaches to Estimating the Performance of LWR Steel Containment Buildings Subject to Severe Accident Loads. Proc. NRC/MITI Technical Information Exchange Workshop, Tokyo, Japan.

Miller, J. D., and Clauss, D. B. (1988). Evaluation of the Performance of the Sequoyah Unit 1 Containment Under Conditions of Severe Accident Loading. Proc. 4th Workshop on Containment Integrity, Arlington, Virginia, pp. 571–588.

MARC Analysis Research Corporation (1983). MARC General Purpose Finite Element Program, Version K.2, User Information Manuals, Volumes A–D, Palo Alto, California.

Greimann, L., Fanous, F., and Bluhm, D. (1984). Final Report, Containment Analysis Techniques, A State-of-the-Art Summary. NUREG/CR-3653, Ames Laboratory, Iowa State University, Ames, Iowa.

Reese, R. T., and Horschel, D. S. (1985). Design and Fabrication of a 1:8-Scale Steel Containment Model. NUREG/CR-3647, SAND84-0048, Sandia National Laboratories, Albuquerque, New Mexico.

Failure Pressure	4° Model	4° Model @ T.	90° Model	90° Model @ T.
Minimum	71	64 @ 311° F	82	76 @ 321° F
Mean	84	74 @ 319° F	83	77 @ 322° F
Maximum	96	85 @ 328° F	85	78 @ 323° F

Table 1: General Shell Analysis Results, *psig*

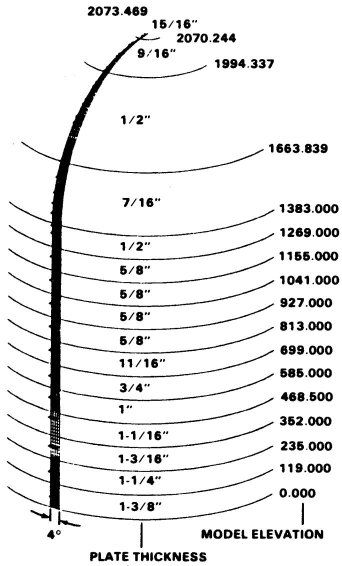

Figure 1: 4° Model

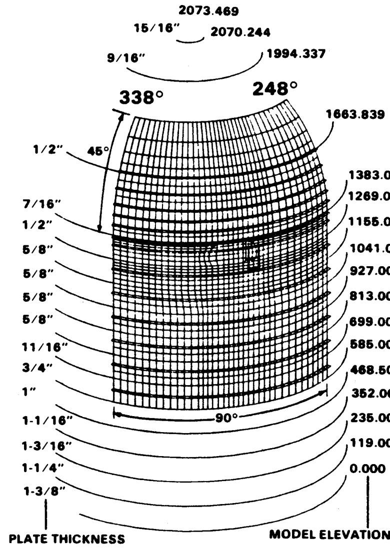

Figure 2: 90° Model

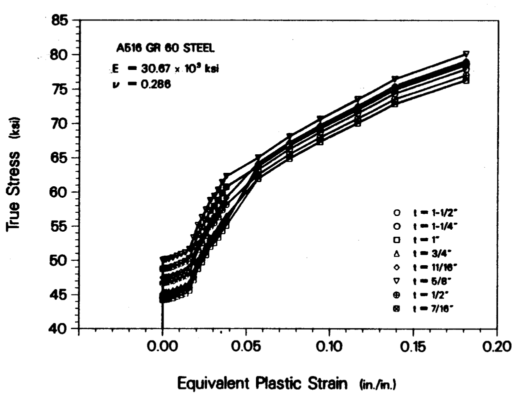

Figure 3: Thickness-Specific Material Properties

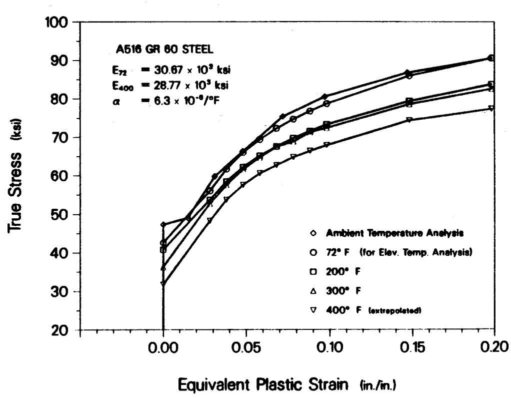

Figure 4: Elevated-Temperature Material Properties

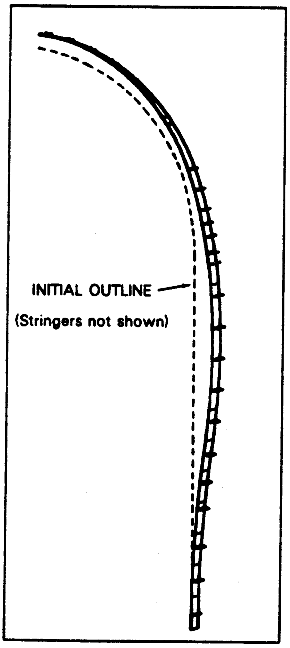

Figure 5: Deformed Shape of the 4° Model at High Pressure

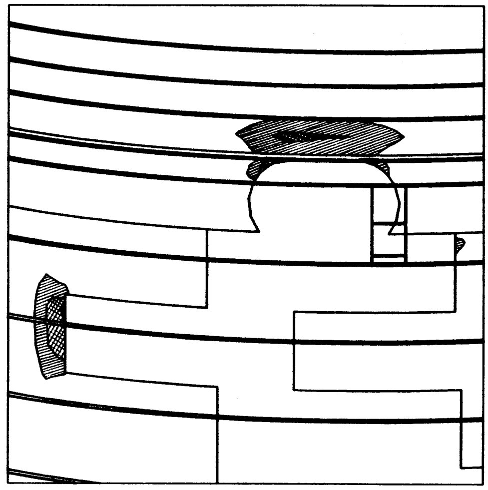

Figure 6: Maximum Strain Locations at High Pressure in the 90° Model

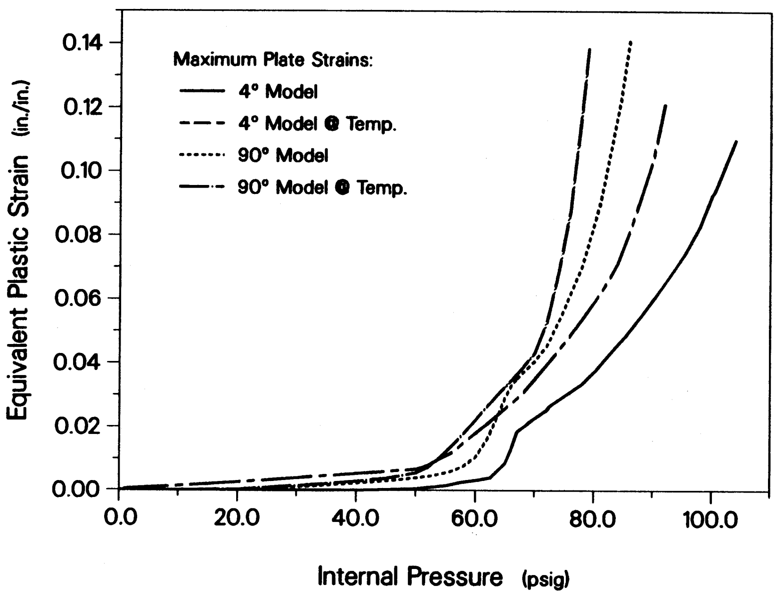

Figure 7: Peak Calculated Strain Histories